

The Crystal Structures of Free Radical Salts and Complexes.
IX. The Crystal Structure and Electrical and Magnetic Properties of
[1,2-Di(*N*-ethyl-4-pyridinium)ethane]₂⁴⁺(7,7,8,8-Tetracyanoquinodimethane)₅⁴⁻

BY G. J. ASHWELL,* D. D. ELEY, S. C. WALLWORK, M. R. WILLIS, G. D. WELCH AND J. WOODWARD

Department of Chemistry, University of Nottingham, Nottingham NG7 2RD, England

(Received 20 December 1976; accepted 22 January 1977)

The crystal structure, electrical conductivity and paramagnetic susceptibility of [1,2-di(*N*-ethyl-4-pyridinium)ethane]₂⁴⁺(7,7,8,8-tetracyanoquinodimethane)₅⁴⁻, (DEPA)₂⁴⁺(TCNQ)₅⁴⁻, are reported. The complex is triclinic, space group *P* $\bar{1}$, with $a = 8.194$, $b = 14.956$, $c = 16.238$ Å, $\alpha = 107.563$, $\beta = 97.25$, $\gamma = 88.26^\circ$, $Z = 1$. The TCNQ's are stacked plane-to-plane in columns with the negative charge delocalized. Anisotropic conductivities are discussed in terms of the crystal structure. Paramagnetic susceptibility measurements on single crystals of (DEPA)₂⁴⁺(TCNQ)₅⁴⁻ show singlet–triplet behaviour.

Introduction

The radical anion salts of TCNQ exhibit some of the highest conductivities known for organic materials; metallic behaviour occurs in several complexes. The complex salt 1,2-di(*N*-ethyl-4-pyridinium)ethylene-(TCNQ)₄, (DEPE)₂²⁺(TCNQ)₄²⁻, crystallizes in two forms: a highly conducting form with $\sigma_{RT} = 150$ – 2200 Ω^{-1} cm⁻¹ (Ashwell, Eley & Willis, 1976; Ashwell, Eley, Willis & Woodward, 1977) and a semiconducting form with $\sigma_{RT} \sim 10^{-3}$ Ω^{-1} cm⁻¹ (Ashwell, Eley, Fleming, Wallwork & Willis, 1976). In an attempt to find other highly conducting complexes the crystal structures and electrical properties of bipyridinium–TCNQ complexes are at present under investigation. In this communication the crystal structure, electrical conductivity and paramagnetic susceptibility are reported of (DEPA)₂⁴⁺(TCNQ)₅⁴⁻, a complex of unusual stoichiometry.

Experimental

Crystal data

(C₁₆H₂₂N₂)₂(C₁₂H₄N₄)₅, $M_r = 1505.6$. Triclinic, $a = 8.194$ (8), $b = 14.956$ (4), $c = 16.238$ (7) Å, $\alpha = 107.563$ (7), $\beta = 97.25$ (3), $\gamma = 88.26$ (4)°; $U = 1882.1$ Å³, $Z = 1$, $D_c = 1.320$ g cm⁻³; $F(000) = 784$. Mo $K\alpha$ ($\lambda = 0.71069$ Å), $\mu = 0.90$ cm⁻¹. Space group *P* $\bar{1}$ (assumed).

Black plates of the complex were deposited when a warm acetonitrile solution (200 ml) of TCNQ (0.3 g) was added to an aqueous solution (10 ml) of 1,2-di(*N*-ethyl-4-pyridinium)ethane diiodide (0.17 g) and al-

lowed to cool slowly. The space group and cell dimensions were obtained initially from oscillation and Weissenberg photographs with Cu $K\alpha$ radiation. The cell constants were subsequently refined on a Hilger & Watts computer-controlled, four-circle diffractometer. Intensities were collected from a crystal $0.13 \times 0.26 \times 0.61$ mm with a $\theta/2\theta$ scan, a scintillation counter and Mo $K\alpha$ radiation. No absorption corrections were made. The intensities were corrected for Lorentz and polarization factors.

Measurement of the electrical conductivity and magnetic susceptibility was carried out as reported previously (Ashwell, Eley, Willis & Woodward, 1977).

Structure determination

The structure was solved from a Patterson synthesis and refined by block-diagonal least squares with 3470 significant reflexions [$I > 3\sigma(I)$]. Refinement of the positional and isotropic thermal parameters of the non-hydrogen atoms, with unit weights, gave $R = 0.096$. Positional parameters of the H atoms were calculated from the coordinates of the C atoms and confirmed by a difference synthesis. The coordinates of the ethyl H atoms were not obvious from the difference map and so were not included in the least-squares calculations. The failure of attempts to locate them is presumed to be due to hindered rotation of the alkyl C atoms about the C–C and C–N single bonds. The lengths of these bonds are clearly erroneous. Block-diagonal, least-squares refinement of the non-hydrogen atoms with anisotropic thermal parameters and the weighting scheme, $w = 1/\{1 + [(|F_o| - A)/B]^2\}$ where $|F_o|$ is on the absolute scale and A and B are equal to 11 gave $R = 0.080$. The H atoms were given isotropic tem-

* Address for 1977: Department of Chemistry, University of Queensland, Brisbane, Qld 4067, Australia.

Table 1. *Final positional parameters* ($\times 10^4$)

The figures in parentheses indicate standard deviations.

	<i>x</i>	<i>y</i>	<i>z</i>		<i>x</i>	<i>y</i>	<i>z</i>
C(1)	70 (5)	569 (3)	1127 (3)	C(30)	3631 (6)	2486 (3)	5338 (3)
C(2)	-599 (5)	-333 (3)	1045 (3)	C(31)	1920 (5)	4083 (3)	-1310 (3)
C(3)	351 (6)	-1098 (3)	940 (3)	C(32)	1535 (6)	3194 (3)	-1874 (3)
C(4)	2064 (5)	-1046 (3)	893 (3)	C(33)	442 (7)	3075 (3)	-2616 (3)
C(5)	2741 (5)	-148 (3)	973 (3)	C(34)	52 (6)	4695 (3)	-2268 (3)
C(6)	1779 (6)	616 (3)	1082 (3)	C(35)	1154 (6)	4841 (3)	-1524 (3)
C(7)	-929 (6)	1357 (3)	1223 (3)	C(36)	-1407 (7)	3681 (4)	-3629 (4)
C(8)	-346 (6)	2256 (3)	1259 (3)	C(37)	-513 (8)	3877 (4)	-4339 (3)
C(9)	-2652 (6)	1315 (3)	1249 (3)	C(38)	3069 (6)	4228 (4)	-496 (3)
C(10)	3073 (5)	-1842 (3)	786 (3)	C(39)	2247 (6)	3994 (4)	209 (3)
C(11)	2435 (6)	-2740 (4)	685 (3)	C(40)	3379 (6)	4142 (3)	1045 (3)
C(12)	4779 (6)	-1801 (3)	739 (3)	C(41)	4070 (7)	3382 (4)	1280 (3)
C(13)	1727 (6)	1443 (3)	3189 (3)	C(42)	5110 (7)	3523 (4)	2035 (4)
C(14)	1061 (6)	558 (3)	3122 (3)	C(43)	4782 (7)	5134 (3)	2360 (3)
C(15)	2020 (5)	-219 (3)	3022 (3)	C(44)	3766 (6)	5026 (3)	1610 (3)
C(16)	3725 (5)	-167 (3)	2974 (3)	C(45)	6765 (9)	4562 (5)	3383 (4)
C(17)	4401 (6)	725 (3)	3049 (3)	C(46)	5837 (9)	4422 (6)	4056 (5)
C(18)	3444 (6)	1495 (3)	3156 (3)	N(1)	78 (6)	2978 (3)	1279 (3)
C(19)	731 (6)	2249 (3)	3296 (3)	N(2)	-4044 (6)	1304 (3)	1278 (3)
C(20)	1366 (6)	3138 (4)	3336 (3)	N(3)	1937 (6)	-3479 (3)	594 (3)
C(21)	-950 (6)	2234 (3)	3376 (3)	N(4)	6174 (5)	-1808 (3)	693 (3)
C(22)	4732 (6)	-963 (3)	2872 (3)	N(5)	1844 (6)	3855 (3)	3368 (4)
C(23)	4113 (6)	-1861 (4)	2802 (3)	N(6)	-2341 (6)	2259 (3)	3449 (3)
C(24)	6461 (6)	-924 (3)	2849 (3)	N(7)	3663 (6)	-2600 (3)	2749 (3)
C(25)	4002 (6)	797 (3)	5110 (3)	N(8)	7842 (6)	-926 (3)	2836 (3)
C(26)	5713 (5)	863 (3)	5051 (3)	N(9)	-93 (6)	1513 (3)	5318 (3)
C(27)	6671 (5)	95 (3)	4951 (3)	N(10)	4150 (7)	3227 (3)	5451 (4)
C(28)	2993 (6)	1585 (3)	5218 (3)	N(11)	-256 (5)	3823 (3)	-2810 (3)
C(29)	1289 (7)	1531 (3)	5262 (3)	N(12)	5467 (6)	4392 (3)	2558 (3)

perature factors of 0.05 \AA^2 and were included in the last few cycles of refinement in fixed calculated positions. Scattering factors were taken from *International Tables for X-ray Crystallography* (1974). The final positional parameters are listed in Table 1. Least-squares planes were calculated for each of the TCNQ moieties and the planar portions of the cation; the results are summarized in Table 2.*

Discussion

Description of the structure

Fig. 1 shows a general view of the structure in which the TCNQ molecules are stacked plane-to-plane in columns in the (010) plane diagonally between the positive directions of *a* and *c*, *i.e.* along [101]. The stacks are held together sideways by van der Waals forces with the closest contacts between stacks, $C \cdots C = 3.247$ and $C \cdots N = 3.376 \text{ \AA}$ (Table 3). In this way layers of TCNQ's are formed parallel to the (010) plane, interleaved by layers of cations.

* Lists of structure factors and anisotropic thermal parameters have been deposited with the British Library Lending Division as Supplementary Publication No. SUP 32451 (35 pp.). Copies may be obtained through The Executive Secretary, International Union of Crystallography, 13 White Friars, Chester CH1 1NZ, England.

Within the columns three types of TCNQ overlap (Fig. 2) are observed with average intermolecular separations of 3.22 ± 0.08 , 3.23 ± 0.05 and $3.26 \pm 0.03 \text{ \AA}$ between *AB*, *BC* and *CC'* respectively. However, when only the quinonoid rings are considered the spacings become 3.20 ± 0.02 , 3.18 ± 0.01 and $3.33 \pm 0.01 \text{ \AA}$ differing from the previous values because of $C-(C \equiv N)_2$ out-of-plane distortions. The dihedral angles between *AB* and *BC* are 2.2° (1.1°) and 0.8° (0.3°) respectively. The figures in parentheses indicate the angles between planes through the quinonoid rings.

The dimensions of the three crystallographically independent types of TCNQ moiety are shown in Fig. 3 and the averaged lengths of chemically similar bonds are summarized in Table 4. The corresponding averaged values for TCNQ(*A*), TCNQ(*B*) and TCNQ(*C*) are, within experimental error, identical and are similar to those observed for TCNQ⁻ (Ashwell, Eley, Wallwork & Willis, 1975). The molecules therefore have the negative charge delocalized with 0.8 - on each TCNQ.

The dimensions of the pyridinium ring (Fig. 3) of the cation are in close agreement with values reported previously for the structures of 1,2-di(*N*-ethyl-4-pyridinium)ethylene(TCNQ)₂ (Ashwell, Eley, Fleming, Wallwork & Willis, 1976), *N,N'*-diethyl-4,4'-

Table 2. Details of molecular planes (x, y, z are fractional atomic coordinates)

TCNQ(A)			TCNQ(C)			
Equations to the planes			Equations to the planes			
Molecule			Molecule			
$0.382x - 1.944y + 15.755z - 8.068 = 0$			$0.424x - 1.562y + 15.664z - 1.634 = 0$			
Quinonoid group			Quinonoid group			
$0.561x - 1.428y + 15.586z - 8.074 = 0$			$0.423x - 1.641y + 15.681z - 1.666 = 0$			
Distances from the planes (Å)			Distances from the planes (Å)			
	Molecule	Quinonoid group		Molecule	Quinonoid group	
C(25)	-0.020	0.001	C(1)	0.045	0.010	
C(26)	-0.059	-0.003	C(2)	0.030	0.002	
C(27)	-0.033	0.003	C(3)	0.024	0.002	
C(28)	-0.041	0.001	C(4)	0.016	-0.006	
C(29)	-0.026	-0.018*	C(5)	0.029	-0.001	
C(30)	-0.003	0.095*	C(6)	0.040	0.005	
N(9)	0.012	-0.007*	C(7)	0.030	-0.011	
N(10)	0.051	0.195*	C(8)	-0.029	-0.077*	
			C(9)	0.005	-0.035*	
			C(10)	0.015	-0.001	
			C(11)	-0.030	-0.039*	
			C(12)	0.008	-0.009*	
			N(1)	-0.093	-0.147*	
			N(2)	-0.008	-0.048*	
			N(3)	-0.078	-0.081*	
			N(4)	-0.004	-0.022*	
TCNQ(B)			Pyridinium ring (A)			
Equations to the planes			Equation to the plane			
Molecule			$6.804x + 3.870y - 10.605z - 4.271 = 0$			
$0.497x - 1.399y + 15.603z - 4.868 = 0$			Distances from the plane (Å)			
Quinonoid group			C(31)	-0.004	C(34)	0.014
$0.415x - 1.559y + 15.666z - 4.847 = 0$			C(32)	0.004	C(35)	-0.004
			C(33)	0.006	N(11)	-0.015
Distances from the planes (Å)			Pyridinium ring (B)			
	Molecule	Quinonoid group	Equation to the plane			
C(13)	-0.008	-0.003	$6.979x + 3.396y - 10.155z - 2.697 = 0$			
C(14)	-0.022	0.002	Distances from the plane (Å)			
C(15)	-0.022	0.005	C(40)	-0.007	C(43)	0.013
C(15)	-0.019	-0.007	C(41)	0.008	C(44)	-0.003
C(17)	0.007	0.000	C(42)	0.001	N(12)	-0.012
C(18)	0.018	0.007				
C(19)	-0.003	-0.003				
C(20)	-0.035	-0.054*				
C(21)	0.039	0.054*				
C(22)	-0.016	0.000				
C(23)	-0.031	0.004*				
C(24)	0.028	0.029*				
N(5)	-0.060	-0.094*				
N(6)	0.081	0.107*				
N(7)	-0.033	0.017*				
N(8)	0.076	0.066*				

* Denotes atoms not defining the plane.

bipyridylum(TCNQ)₄ (Ashwell, Eley, Wallwork & Willis, 1975) and 1,4-di(*N*-pyridiniummethyl)-benzene(TCNQ)₄ (Ashwell, Wallwork, Baker & Berthier, 1975, 1976). The angle between the mean planes through the two pyridinium rings is 2.6°. The angles that these planes make with TCNQ(A) are 62.2 and 60.5°, with TCNQ(B) 63.4 and 61.7° and with TCNQ(C) 62.8 and 61.1° respectively.

Electrical properties

The electrical properties of (DEPA)₂⁴⁺(TCNQ)₃⁴⁻ reflect the molecular packing within the crystal. A

parallel plane-to-plane stacking of the radical anions in columns along [101] gives rise to anisotropy with the highest conductivity in a direction parallel to the stack. The resistivities at 300 K along the long, intermediate and short crystal axes are 25, 18 and 1500 Ω cm respectively. The TCNQ's are stacked plane-to-plane in columns along the intermediate axis. The higher resistivity along the short axis reflects the alternating layers of TCNQ's and cations in this direction.

The temperature dependence of the conductivity along all three crystal directions is isotropic and varies as $\exp(-E_A/kT)$ where $E_A = 0.14 \pm 0.02$ eV.

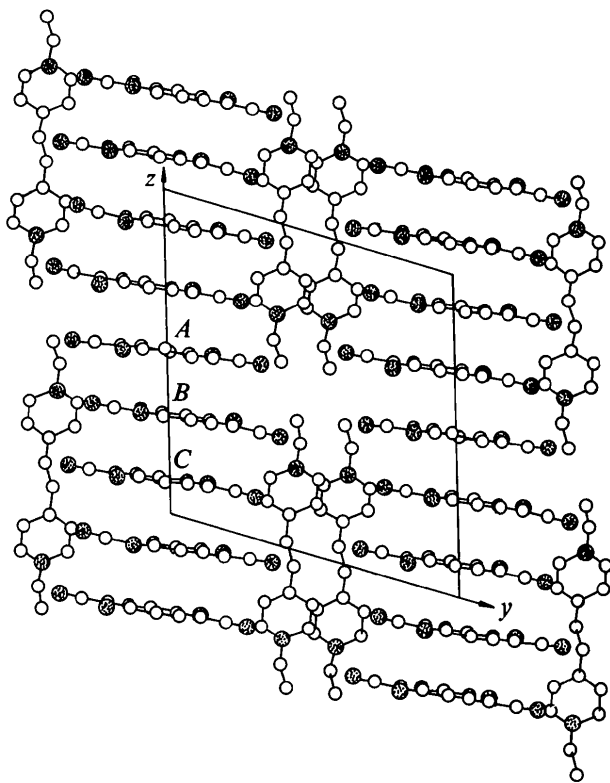


Fig. 1. The structure of $(\text{DEPA})_2^{4+}(\text{TCNQ})_5^{4-}$ projected along *a*.

Magnetic properties

The paramagnetic susceptibility of $(\text{DEPA})_2^{4+}(\text{TCNQ})_5^{4-}$ exhibits singlet-triplet behaviour. A plot of $\log(IT)$ versus reciprocal temperature (Fig. 4), where *I* is the ESR signal intensity, indicates the presence of two activation energies for the formation of magnetically active states, 0.10 eV above 200 K and 0.039 eV below. This unusual behaviour may result from the formation of states with higher multiplicities caused by the interaction of electrons in different environments within the TCNQ stack. Alternatively, a phase change may cause a corresponding transition in the singlet-triplet separation. However, no indications of such a change were found in the conductivity data.

Interpretation of the curvature of the $\log(IT)$ *v.* 10^3 K/*T* plot as arising from a lower activation energy and not a Curie Law contribution to the signal intensity is supported by the behaviour on further cooling. In the region of 100 K the signal intensity decreased markedly before changing to a Curie Law type increase at lower temperatures. The ESR signal consisted of a single narrow resonance down to 100 K, whereas below this temperature two signals of different line-width (~ 5 MHz and ~ 22 MHz) were observed situated at the same *g* factor. The line-widths exhibited only slight anisotropy. The numbers of species giving rise to these signals, estimated from standard DPPH samples, were $1.4 \pm$

Table 3. Short intermolecular contacts (Å)

The figures in parentheses indicate standard deviations.

TCNQ(B)–TCNQ(A)		TCNQ(C)–TCNQ(C)	
C(13 ⁱ)–C(28 ⁱ)	3.272 (7)	C(2 ⁱ)–C(6 ⁱⁱ)	3.368 (7)
C(13 ⁱ)–C(29 ⁱ)	3.393 (7)	C(4 ⁱ)–C(7 ⁱⁱ)	3.338 (7)
C(14 ⁱ)–C(29 ⁱ)	3.321 (6)	TCNQ–cation	
C(16 ⁱ)–C(25 ⁱ)	3.311 (6)	N(1 ⁱ)–C(34 ^{vi})	3.369 (6)
C(17 ⁱ)–C(25 ⁱ)	3.373 (7)	N(1 ⁱ)–C(35 ^{vi})	3.307 (6)
C(17 ⁱ)–C(26 ⁱ)	3.239 (7)	N(1 ⁱ)–C(39 ⁱ)	3.320 (8)
C(18 ⁱ)–C(28 ⁱ)	3.377 (7)	N(1 ⁱ)–C(40 ⁱ)	3.382 (7)
C(18 ⁱ)–C(30 ⁱ)	3.388 (6)	N(1 ⁱ)–C(41 ⁱ)	3.344 (8)
C(24 ⁱ)–C(27 ⁱ)	3.276 (6)	N(2 ⁱ)–C(42 ⁱⁱⁱ)	3.259 (7)
TCNQ(C)–TCNQ(B)		N(3 ⁱ)–C(44 ^{vii})	3.371 (7)
C(1 ⁱ)–C(13 ⁱ)	3.329 (6)	N(4 ⁱ)–C(41 ^{viii})	3.341 (6)
C(1 ⁱ)–C(14 ⁱ)	3.244 (7)	N(5 ⁱ)–C(46 ⁱ)	3.368 (9)
C(2 ⁱ)–C(14 ⁱ)	3.353 (6)	N(7 ⁱ)–C(36 ⁱⁱ)	3.212 (9)
C(3 ⁱ)–C(15 ⁱ)	3.360 (6)	N(7 ⁱ)–C(43 ^{vii})	3.375 (6)
C(4 ⁱ)–C(15 ⁱ)	3.306 (6)	N(8 ⁱ)–C(32 ^{viii})	3.333 (6)
C(4 ⁱ)–C(16 ⁱ)	3.356 (6)	N(9 ⁱ)–C(36 ^{ix})	3.392 (7)
C(5 ⁱ)–C(16 ⁱ)	3.256 (7)	N(10 ⁱ)–C(45 ^x)	3.393 (8)
C(5 ⁱ)–C(17 ⁱ)	3.349 (6)	N(10 ⁱ)–C(46 ^x)	3.363 (10)
C(6 ⁱ)–C(13 ⁱ)	3.274 (7)	Inter-stack	
C(6 ⁱ)–C(18 ⁱ)	3.348 (6)	C(2 ⁱ)–N(4 ⁱⁱⁱ)	3.376 (6)
C(7 ⁱ)–C(19 ⁱ)	3.347 (6)	C(5 ⁱ)–N(2 ^{iv})	3.357 (6)
C(7 ⁱ)–C(21 ⁱ)	3.345 (6)	C(14 ⁱ)–N(8 ⁱⁱⁱ)	3.395 (7)
C(8 ⁱ)–C(19 ⁱ)	3.317 (7)	C(15 ⁱ)–C(27 ^v)	3.282 (7)
C(8 ⁱ)–C(20 ⁱ)	3.364 (6)	C(16 ⁱ)–C(27 ^v)	3.395 (7)
C(10 ⁱ)–C(22 ⁱ)	3.363 (6)	C(22 ⁱ)–C(25 ^v)	3.247 (7)
C(10 ⁱ)–C(23 ⁱ)	3.285 (7)	C(22 ⁱ)–C(26 ^v)	3.396 (7)
C(11 ⁱ)–N(7 ⁱ)	3.321 (7)	C(23 ⁱ)–C(26 ^v)	3.339 (6)
C(12 ⁱ)–C(22 ⁱ)	3.314 (6)	C(24 ⁱ)–C(25 ^v)	3.331 (7)
N(1 ⁱ)–C(20 ⁱ)	3.312 (7)	C(27 ⁱ)–N(9 ^{iv})	3.326 (6)
N(1 ⁱ)–N(5 ⁱ)	3.393 (7)		
N(4 ⁱ)–C(24 ⁱ)	3.328 (6)		

Superscripts indicate equivalent positions as follows:

- | | |
|----------------------------------|----------------------------------|
| (i) x, y, z | (vi) $\bar{x}, 1 - y, \bar{z}$ |
| (ii) $\bar{x}, \bar{y}, \bar{z}$ | (vii) $x, y - 1, z$ |
| (iii) $x - 1, y, z$ | (viii) $1 - x, \bar{y}, \bar{z}$ |
| (iv) $x + 1, y, z$ | (ix) $x, y, z + 1$ |
| (v) $1 - x, \bar{y}, 1 - z$ | (x) $1 - x, 1 - y, 1 - z$ |

0.4×10^{22} for the narrow and $1.1 \pm 0.3 \times 10^{23}$ spins mol^{-1} for the broad resonance.

There was no direct observation of dipolar splitting in $(\text{DEPA})_2^{4+}(\text{TCNQ})_5^{4-}$. However, for two crystal orientations the line-width decreased with increasing temperature thus indicating that any such splitting was exchange-narrowed (Etemad, 1972). This is supported by the fact that two triplet states per unit cell would lead to a rapid exchange narrowing. Unfortunately, the variation with temperature of the line-width was too small to allow a meaningful exchange analysis to be carried out.

When the crystal was mounted with the TCNQ stacking direction parallel to the rotation axis and the magnetic field parallel to either of the other crystal axes, the line-width increased with temperature. Similar behaviour in a related complex has been interpreted (Etemad, 1972) in terms of interchain hopping. In such

a case a plot of $\log \Delta H$ versus reciprocal temperature should have a slope of $J/2k$. However, for $(\text{DEPA})_2^{4+}$ - $(\text{TCNQ})_5^{4-}$, Fig. 5 gives $J = 0.027$ eV which is considerably smaller than either of the values obtained from the $\log(IT)$ v. $10^3 K/T$ plot (Fig. 4). It would therefore appear that this process is complicated by a number of phenomena.

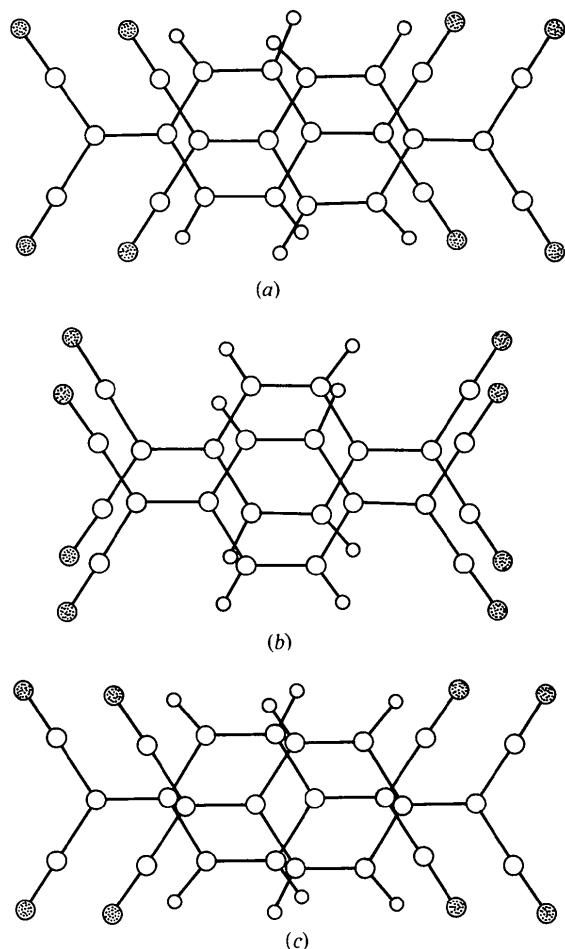


Fig. 2. Nearest-neighbour overlap. (a) $\text{TCNQ}(A)$ - $\text{TCNQ}(B)$, (b) $\text{TCNQ}(B)$ - $\text{TCNQ}(C)$ and (c) $\text{TCNQ}(C)$ - $\text{TCNQ}(C')$.

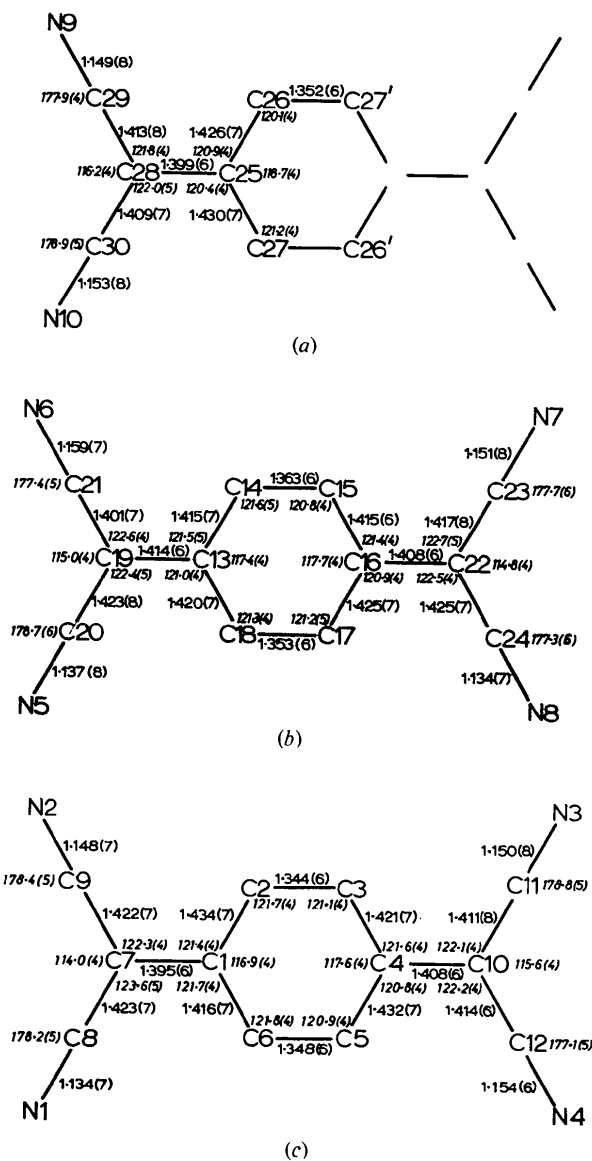


Fig. 3. Bond lengths (Å) and angles ($^\circ$) (with their standard deviations in parentheses) for (a) $\text{TCNQ}(A)$, (b) $\text{TCNQ}(B)$, (c) $\text{TCNQ}(C)$.

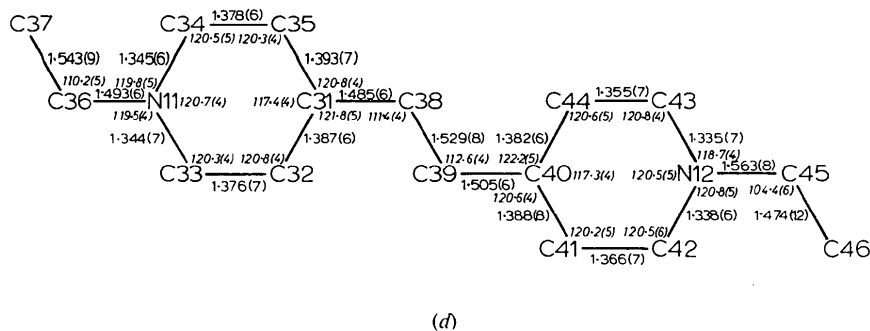
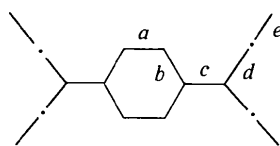


Fig. 3 (cont.). (d) The 1,2-di(*N*-ethyl-4-pyridinium)ethane cation.

Table 4. Comparison of mean bond lengths (Å, uncorrected for libration)



Bond	a	b	c	d	e
*TCNQ [•]	1.346	1.448	1.374	1.440	1.138
†TCNQ ⁻	1.362	1.424	1.413	1.417	1.149
TCNQ(A)	1.352	1.428	1.399	1.411	1.151
TCNQ(B)	1.358	1.419	1.411	1.417	1.145
TCNQ(C)	1.346	1.426	1.402	1.418	1.147
Mean of A,B,C	1.352 (7)	1.423 (7)	1.405 (8)	1.416 (8)	1.147 (9)

* Long, Sparks & Trueblood (1965).

† Ashwell, Eley, Wallwork & Willis (1975) and references therein.

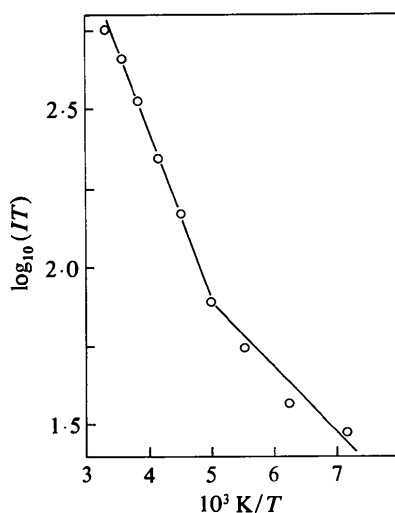


Fig. 4. $\log_{10}(IT)$ versus reciprocal temperature for single crystals of $(\text{DEPA})_2^{4+}(\text{TCNQ})_2^{4-}$ where I is the ESR signal intensity.

The principal elements of the g tensor (Chesnut & Phillips, 1961) are 2.0030 (3), 2.0037 (3) and 2.0028 (3) at 300 K for g_x , g_y and g_z respectively. The value most closely associated with the TCNQ stacking direction, g_z , is closest to the free electron value. This phenomenon has been observed in a number of TCNQ complexes (Chesnut & Phillips, 1961; Faucher & Robert, 1974; Tomkiewicz, Scott, Tao & Title, 1974) and reflects the greater delocalization in this direction.

We thank Professor T. J. King for assistance with the diffractometry, Miss G. Owens for assistance with

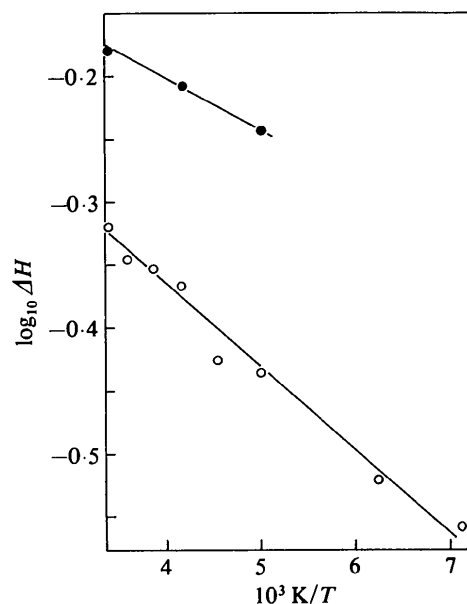


Fig. 5. $\log_{10}(\Delta H)$ versus reciprocal temperature for single crystals of $(\text{DEPA})_2^{4+}(\text{TCNQ})_2^{4-}$ where ΔH is the line-width. (●) H_0 approximately parallel to the b axis and (○) H_0 approximately parallel to the a axis.

the magnetic measurements and the SRC for contributing to the cost of the diffractometer and for the award of research studentships to JW and GDW.

References

- ASHWELL, G. J., ELEY, D. D., FLEMING, R. J., WALLWORK, S. C. & WILLIS, M. R. (1976). *Acta Cryst.* **B32**, 2948–2952.
- ASHWELL, G. J., ELEY, D. D., WALLWORK, S. C. & WILLIS, M. R. (1975). *Proc. Roy. Soc. A* **343**, 461–475.
- ASHWELL, G. J., ELEY, D. D. & WILLIS, M. R. (1976). *Nature, Lond.* **259**, 201–202.
- ASHWELL, G. J., ELEY, D. D., WILLIS, M. R. & WOODWARD, J. (1977). *Phys. Stat. Sol.* To be published.
- ASHWELL, G. J., WALLWORK, S. C., BAKER, S. R. & BERTHIER, P. I. C. (1975). *Acta Cryst.* **B31**, 1174–1178. Erratum: (1976). *Acta Cryst.* **B32**, 2920.
- CHESNUT, D. B. & PHILLIPS, W. D. (1961). *J. Chem. Phys.* **35**, 1002–1012.
- ETEMAD, S. (1972). PhD Thesis, Univ. of Pennsylvania.
- FAUCHER, J.-P. & ROBERT, H. (1974). *C. R. Acad. Sci. Paris, Sér. B*, **270**, 174–177.
- International Tables for X-ray Crystallography* (1974). Vol. IV. Birmingham: Kynoch Press.
- LONG, R. E., SPARKS, R. A. & TRUEBLOOD, K. N. (1965). *Acta Cryst.* **18**, 932–939.
- TOMKIEWICZ, Y., SCOTT, B. A., TAO, L. J. & TITLE, R. S. (1974). *Phys. Rev. Lett.* **32**, 1363–1366.